Enabling Relative Localization for Nanodrone Swarm Platooning

Wei Sun

Abstract—**Nanodrone swarm is formulated by multiple lightweight and low-cost nanodrones to perform the tasks in very challenging environments. Therefore, it is essential to estimate the relative position of nanodrones in the swarm for accurate and safe platooning in inclement indoor environment. However, the vision and infrared sensors are constrained by the line-of-sight perception, and instrumenting extra motion sensors on drone's body is constrained by the nanodrone's form factor and energy-efficiency.**

This paper presents the design, implementation and evaluation of RFDrone, a system that can sense the relative position of nanodrone in the swarm using wireless signals, which can naturally identify each individual nanodrone. To do so, each lightweight nanodrone is attached with a RF sticker (i.e., called RFID tag), which will be localized by the external RFID reader in the inclement indoor environment. Instead of accurately localizing each RFID-tagged nanodrone, we propose to estimate the relative position of all the RFID-tagged nanodrones in the swarm based on the spatial-temporal phase profiling. We implement an end-to-end physical prototype of RFDrone. Our experimental results show that RFDrone can accurately estimate the relative position of nanodrones in the swarm with average relative localization accuracy of around 0.95 across x, y and z axis, and average accuracy of around 0.93 for nanodrone swarm's geometry estimation.

I. INTRODUCTION

Unmanned aerial vehicles (UAVs) become popular for performing the severe tasks (e.g., rescuing lives during the disasters [59] and package delivery [46]), enhancing the performance of cellular network [38, 13] and proliferating the entertainment industry [21], which exhibits the exceptional agility and flexibility of the drones [52]. For example, Intel, SKYMAGIC [4], Verity Studios and ElevenPlay have created dazzling drone shows, where each drone is equipped with the LED to display the animations in the sky. However, these UAVs need to be instrumented with different kinds of sensors atop the UAVs to sense the environment and assist the path planning for optimal navigation and safe platooning. The drone is usually equipped with IMU sensors to track the drone orientation and flying path, which is not accurate due to the drift of these IMU sensors [23]. Recently, SafetyNet [25] uses four GPS receivers atop the drone to track the drone orientation in the outdoor scenario. Note, these bulky and power-hungry sensors hinder the proliferation of drone's deployment and development in the cluttered environment.

Recently, the lightweight and small form-factor nanodrone (e.g., quadrotor or quadcopter) is designed, unlike the large industrial drones (e.g., Amazon drones and DJI drones have orders of magnitude larger size), which can just fit in our palm as shown in Fig. 1. The nanodrone is as small as 22x22x20 mm (e.g., Mini Drone FY804 [5]) and 70x48x35 mm (e.g., Holyton HT02 Mini Drone [6]), which can enable it to traverse through the small, tight and narrow space such as plant canopies and crevices to perform the tasks. So, we can use nanodrones to perform the sensing tasks in some severe environments (e.g., forests and disaster sites), which cannot be easily accessible by humans. However, we cannot instrument different sensors on the nanodrone due to its small size and limited power, thereby the ability of nanodrone performing the tasks is limited. Inspired by the concept of crowdsourcing [12], multiple nanodrones can formulate a nanodrone swarm for emergency response and hazard detection in urban settings [31]. It is necessary for the nanodrone swarm to formulate an accurate geometry of swarm pattern for safe and accurate platooning [14], such that the sensing tasks can be efficiently performed.

Fig. 1: The nanodrone with size of 70x48x35mm, fitting in the palm.

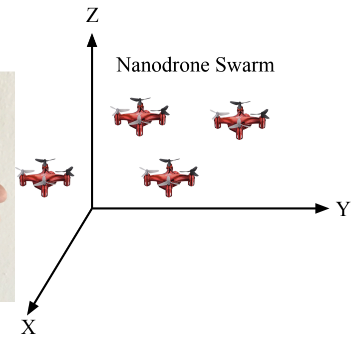

Fig. 2: Example of nanodrone swarm with four nanodrones flying in the 3D space.

To sense the relative position of nanodrones in the swarm as shown in Fig. 2, the straightforward idea is to use the vision-based sensors (e.g., stereo cameras) and ranging-based LiDAR sensors [30]. However, these advanced sensors cannot work properly in non-line-of-sight settings and are not cost-effective [32], especially in the presence of airborne obscurants (e.g., dust, fog and smoke). Alternatively, RF-based sensing techniques have been widely developed in indoor localization, which can be leveraged to sense the relative position of nanodrones in the swarm. But, it is not possible to instrument these bulky and power-hungry RF radios or motion sensors on the nanodrone.

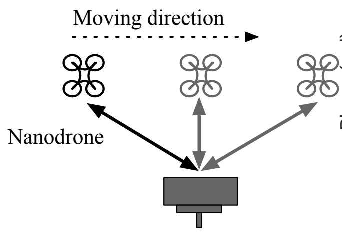

Fig. 3: The nanodrone is moving from left to right in front of the reader's antenna.

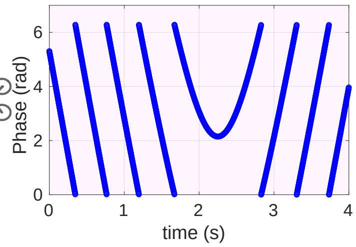

Fig. 4: Phase readings over time, when the RFID-tagged nanodrone is moving from left to right in front of the reader's antenna.

As the proliferation of Radio Frequency IDentification (RFID) technology, they are widely used in different kinds of sensing tasks such as indoor localization [33, 56, 35] and gesture recognition [58, 50, 48, 61]. The commodity passive RFID tags are battery-free, ubiquitous, low-cost and small form-factor, enabling them to be the good fit to enhance the nanodrone swarm applications. Therefore, we can just attach the commodity passive RFID tag to each nanodrone in the swarm, such that we can sense the RFID-tagged nanodrone's relative position in the swarm by analysing the backscattered signals from each RFID tag. However, simply applying the state-of-the-art RFID-based localization techniques [56, 33, 35] cannot accurately localize each individual RFID-tagged nanodrone in the swarm over 3D space without any hardware modifications.

In this paper, we propose RFDrone, a system that can accurately sense the relative position of the nanodrones in the swarm, using commodity passive RFID tags. Specifically, we attach commodity passive RFID tag to each of nanodrones in the swarm. Then, the relative position of the naodrones in the swarm is sensed through the spatial-temporal phase profile of the backscattered signals from the RFID-tagged nanodrone.

Our main idea is to leverage the linear relationship between phase readings and the reader-tag distance. The phase readings will decrease/increase as the reader-tag distance decreases/increases. So, when the RFID-tagged nanodrone moves from left to right in front of the reader's antenna as shown in Fig. 3, there is a trough zone in the phase profile as shown in Fig. 4. Thus, we can estimate the relative position of RFID-tagged nanodrones based on the trough zone of spatial-temporal phase profile. Specifically, in the 3D space, the relative position along x axis is estimated based on the time ordering of trough's lowest point, and the relative position along y axis is estimated based on the phase changing rate [22, 49]. However, this does not work in our scenario, since the above approach assumes all the tags have the same height along z axis. Moreover, we cannot predict the relative position of nanodrones along z axis based on the above approach. Different from the scenarios proposed in STPP [49] and Taggo [22], the RFID-tagged nanodrone swarm can fly around in the 3D space, which can be harnessed for relative position estimation. Specifically, we can leverage the time ordering of trough's lowest point for relative position estimation, as the nanodrone swarm flies around.

Contributions. We prototype RFDrone with commodity passive RFID tags using software defined USRP N210 as the RFID reader, where we just extract the backscattered channel to profile the spatial-temporal phase readings for each RFID-tagged nanodrone in the swarm. Our experimental results show the average relative localization accuracy of around 0.95 across x, y and z axis, and average accuracy of around 0.93 for nanodrone swarm's geometry estimation. We discuss the limitation and future work of RFDrone in Sec. **??**. RFDrone's contributions are three-fold as follows:

- To the best of our knowledge, RFDrone is the first system that can accurately sense the relative position of the nanodrone in swarm with commodity passive RFIDs in the inclement indoor environment.
- Second, we propose to estimate the relative positions of the nanodrones in the swarm based on spatial-temporal phase profiling.
- At last, we built and implemented the RFDrone with commodity passive RFID system and demonstrated its ability and accuracy to sense the relative position of nanodrones in the swarm in cluttered indoor environment and outdoor environment.

In what follows, we first introduce the related work in Sec. II. Then, we present the overview of RFDrone's design in Sec. III. The details of RFDrone's design will be shown in Sec. IV, which will be followed by implementation and evaluation in Sec. V and experimental results in Sec. VI. At last, we present the limitations and future development opportunities of RFDrone in Sec. **??**, and conclude our paper in Sec. VII.

II. Related Work

A. RFID-Based Robotic Applications

Radio Frequency IDentification (RFID) is a mature technology that has been widely used in retail, manufacturing and warehousing [56, 55, 57, 58, 54, 27] for identification due to its low cost, small form factor and batter-free. Recently, we notice that the advances in RFID localization have proliferated its applications in robotic grasping [11, 10, 42, 26, 29, 18, 16, 19, 17] and localization [57, 34, 33, 47, 49]. However, these systems only focus on one robot's manipulation. In contrast, RFDrone demonstrates, for the first time, how spatial-temporal phase profiling of backscattered signals can be leveraged to achieve relative localization of nanodrone swarm. More importantly, we cannot simply apply the existing RFID-based sensing techniques to accurately localize each individual nanodrone in the swarm over the 3D space without hardware modifications on RFID reader or tag.

B. Drone Swarm Tracking and Localization

Nanodrone swarm can leverage multiple nanodrones' capabilities to improve the overall system's resilience and accelerate the task performing in aerial photography, topography and

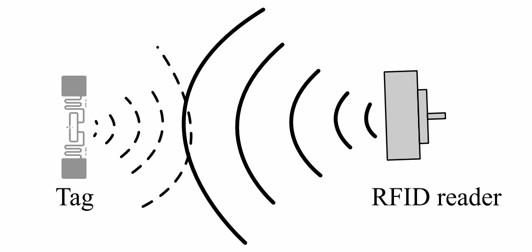

Fig. 5: The commodity passive RFID system consists of reader and RFID tags, which is compatible with EPC Gen2 standard.

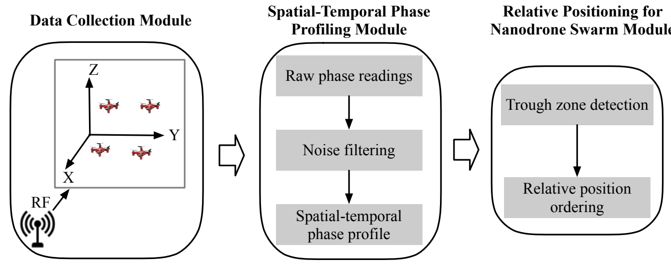

Fig. 6: RFDrone's workflow operation.

delivery [9, 36, 24, 40, 36, 8, 39, 41]. To maximum embrace the nanodrone swarm's capability, it is important to recognize the relative position of nanodrones in the swarm. The straightforward idea is to use vision or infrared sensors to sense the relative positions of drone swarm [45, 44, 43, 37, 60, 15]. However, these vision or infrared sensors are constrained by the line-of-sight perception. Recent studies [51, 20, 53, 25] mount the motion sensors on the robot to sense the relative position among the drones in the swarm. However, it is impossible to instrument these bulky and power-hungry sensors on the nanodrone with Size, Weight and Power (SWaP) constraints. In contrast, RFDrone uses low-cost, battery-free, ubiquitous and small form-factor RFID tags to sense the relative positions among the nanodrones in the swarm by profiling the spatial-temporal phase readings from backscattered signals.

III. RFDrone's Overview

In this section, we present the overview of our proposed RFDrone. As shown in Fig. 6, RFDrone consists of three main modules: data collection module, spatial-temporal phase profiling module and relative positioning for nanodrone swarm module.

When the nanodrone swarm flies around in the 3D space, the reader will receive the backscattered signals from each RFID-tagged nanodrone. The extracted phase readings from the backscattered signals will be preprocessed with the Savitzky-Golay filter to eliminate the noisy points. The preprocessed phase readings over time will be used to create the spatial-temporal phase profile. Specifically, we will create three spatial-temporal phase profiles, when the nanodrone swarm flies along x, y and z axis. Note that each spatial-temporal phase profile will have a trough zone due to the relationship between the phase and reader-tag distance, which will be leveraged to predict the relative positions of nanodrones in the swarm. After we obtain the spatial-temporal phase profiles along x, y and z axis, we need to detect the trough zone in the profile. To do so, we use the algorithm proposed in Taggo [22] to detect the trough zone with only one run of scanning the phase profile, which is proved to be more efficient than the time-consuming Dynamic Time Warping (DTW) [49]. Then, we can obtain the time ordering of the trough's lowest point, which can be leveraged to predict the relative position of the nanodrones in the swarm.

In the following section, we will illustrate RFDrone's design in more details. First, we will show the relative position estimation across x, y and z axis (§ IV-A) for the nanodrones in the swarm. Then, we create the spatial-temporal phase profiles using the phase readings (§ IV-B). At last, we will present relative positioning for nanodrone swarm based on the spatial-temporal phase profiles (§IV-C).

IV. RFDrone's Design

In this section, we will present RFDrone's design in details. We start from the relative position estimation of nanodrones in the swarm along x, y and z axis.

A. Relative Position Estimation of Nanodrones in 3D Space

To find the relative position of nanodrones in the swarm, we can use the linear relationship between the phase of backscattered signals and the reader-tag distance as follows:

$$\theta = (\frac{2\pi * 2d}{\lambda} + \mu) \ mod \ 2\pi \tag{1}$$

where θ is the phase of backscattered signals, λ is the wavelength, d is the distance between reader and tag and μ indicates the phase shift due to the noise. As illustrated in the introduction section, the phase profile will exhibit a trough zone when the RFID-tagged nanodrone moves from left to right in front of the reader's antenna. Therefore, the relative position of two nanodrones along x axis can be estimated based on the time when the lowest point of trough zone has been achieved. To see this clearly, we do the experiments with a nanodrone swarm consisting of two nanodrones. The nanodrone 1 and 2 move from left to right in front of reader's antenna along the x axis as shown in Fig. 7, where nanodrone 1 is at right of nanodrone 2. So, nanodrone 1 is closer to reader's antenna in comparison to nanodron 2. If we plot the phase profile of RFID-tagged nanodrone 1 and 2 as shown in Fig. 8, we can see two trough zones in the phase profiles of nanodrone 1 and 2. Moreover, the lowest point of trough in the phase profile from nanodrone 1 will be at the left of lowest point of trough in the phase profile from nanodrone 2. This is because nanodrone 1 is closer to the reader's antenna in comparison to the nanodrone 2. Therefore, we can predict the relative position of nandorone 1 and 2 based on the time ordering of the lowest point of trough in their phase profiles.

After we figure out the relative position of two nanodrones along x axis, the problem becomes how we can predict the

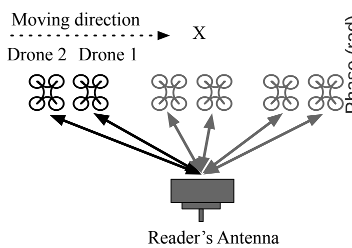

Fig. 7: Two nanodrones are moving from left to right in front of the reader's antenna along x axis.

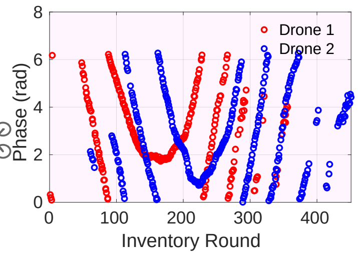

Fig. 8: Spatial and temporal phase profile from two nanodrones, indicating the relative position of them along x axis based on the time when the trough's lowest point has been achieved.

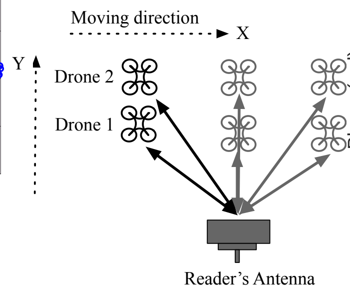

Fig. 9: Two nanodrones are moving from left to right in front of the reader's antenna along x axis.

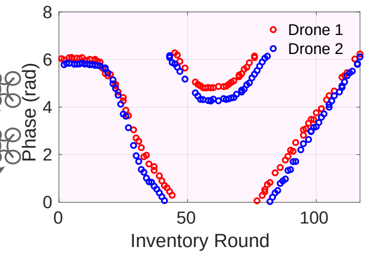

Fig. 10: Spatial and temporal phase profile from two nanodrones, indicating the relative position of them along y axis based on the value of trough's lowest point.

relative position of nanodrones in the swarm along y axis. To do so, we put two nanodrones in front of reader's antenna with same x coordinates and different y coordinates (e.g., y coordinate of nanodrone 1 is smaller than nanodrone 2) as shown in Fig. 9, where two nanodrones will move along x axis. Obviously, nanodrone 1 is closer to the reader's antenna. Then, we plot the phase readings of two nanodrones over time as shown in Fig. 10. Since two nanodrones have the same x coordinates, we cannot predict their relative positions based on time ordering of trough's lowest point in the phase profile. As we can see, the lowest points of trough from the phase profiles of nanodrone 1 and 2 will be achieved simultaneously. However, we can see that the lowest point of trough in the phase profile from nandrone 1 is smaller than the lowest point of trough in the phase profile from nanodrone 2. This is because nanodrone 1 is closer to the reader's antenna. Mathematically, in this scenario, the phase changing rate over time can be expressed in the following equation as illustrated in Taggo [22]:

$$R_p = \frac{d\theta}{dt} = \frac{4\pi}{\lambda} \frac{v^2 t + v x_0}{\sqrt{(x_0 + vt)^2 + y_0^2}} \tag{2}$$

where v is the moving speed of the RFID-tagged object, λ is the signal wavelength and (x_0, y_0) indicates the coordinates of the object. As we can see, the smaller coordinate indicates the larger phase changing rate, which is in accord with our above observation in the experiment. Therefore, we can predict the relative position of nanodrones along y axis based on the value of trough's lowest point (or phase changing rate) in the phase profile.

Note that the above discussion assumes that the nandorones in the swarm have the same height along z axis. To predict the relative position of nanodrones in 3D space, we need to consider different heights of nanodrones along z axis. Fortunately, the time ordering for relative position estimation along x axis will not be affected by the different heights of the nanodrones along z axis, since the nanodrone closer to the reader's antenna along x axis will always achieve the lowest point of the trough in the phase profile earlier than the other

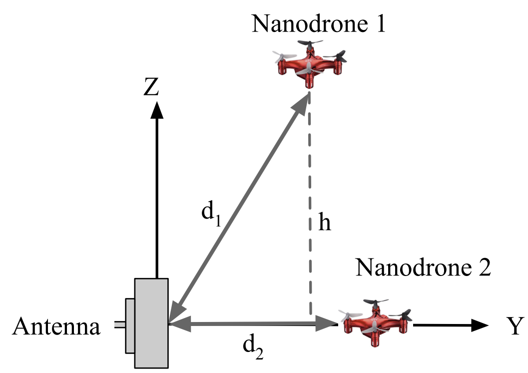

Fig. 11: Nanodrone 1 is closer to the reader's antenna along y axis in comparison to naodrone 2. Both of nanodrone 1 and 2 have the same x coordinate. However, the distance between nanodrone 1 and reader's antenna (i.e., d_1) is larger than the distance between nanodrone 2 and reader's antenna (i.e., d_2) due to the larger height (i.e., h) of nanodrone 1 along z axis.

nanodrones. However, the different height of nanodrone along z axis will affect estimation of nanodrone's relative position along y axis. As shown in Fig. 11, let's assume two RFID-tagged nanodrones have the same x coordinates. Nanodrone 1 has smaller y coordinate and larger z coordinate in comparison to the nanodrone 2. In this case, if we plot the phase readings of two nanodrones and use the above discussed approaches to estimate the nanodrone's relative positions along y axis, we will disorder their relative position along y axis based on the value of trough's lowest point (or phase changing rate). This is because the distance (i.e., d_1) between nanodrone 1 and reader's antenna is larger than distance (i.e., d_2) between nanodrone 2 and reader's antenna due to the larger height (i.e., h) of nanodrone 1.

Since our goal is to estimate the relative position of nanodrones along x, y and z axis in 3D space, the above discussion indicates that we cannot predict the relative position along y axis without considering the height of nanodrones along z axis. Moreover, we need to predict the relative position of the

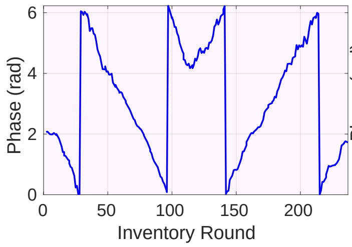

Fig. 12: Raw phase readings over inventory rounds, which includes a trough zone from 100 to 150 inventory rounds.

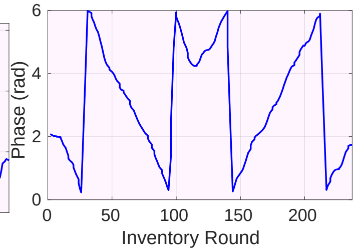

Fig. 13: Phase readings over inventory rounds after we apply Savitzky-Golay filter on raw phase readings to eliminate the noisy points.

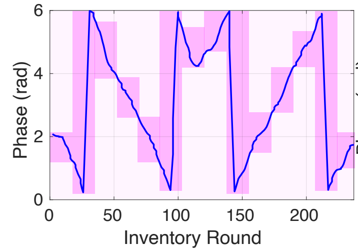

Fig. 14: Trough zone detection with the sliding window on phase readings over inventory rounds.

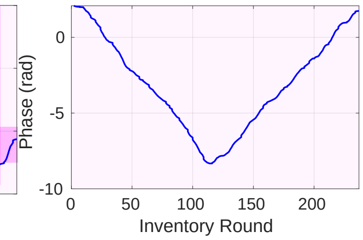

Fig. 15: Phase readings over inventory rounds after we splice the adjacent parts together.

nanodrones along z axis. To this end, we profile the spatial-temporal phase along x, y and z axis separately to achieve relative position estimation of the nanodrones in the swarm.

B. Spatial-Temporal Phase Profiling

To predict the relative positon of nanodrones in the swarm along x, y and z axis, the nanodrone swarm will fly along x, y and z axis to obtain the time ordering of trough's lowest point along x , y and z axis in the spatial-temporal phase profile. When the nanodrone swarm is flying along a specific axis, the time ordering of trough's lowest point just depends on the nanodrone's coordinates along that axis.

However, the phase readings of backscattered signals is noisy due to the cluttered environment and nanodrone's body vibration. Thus, we need to preprocess the raw phase readings to obtain the clean spatial-temporal phase profile. To do so, we apply the Savitzky-Golay filter on the raw phase readings to mitigate the noisy points, which will help us to detect the trough zone and recognize its lowest point for relative position estimation. As shown in Fig. 12, we show the raw phase readings over time, when RFID-tagged nanodrone is flying along x axis in front of reader's antenna. After we apply the Savitzky-Golay filter on the phase readings, we can see the smooth phase readings over time as shown in Fig. 13.

C. Relative Positioning for Nanodrone Swarm

After we obtain the spatial-temporal phase profile for each nanodrone in the swarm, we need to detect the trough zone for time ordering of trough's lowest point that can help us to relatively localize the position of nanodrones.

1) Trough Zone Detection.: It is important to efficiently and accurately detect the trough zone in the spatial-temporal phase profile for relative localization. The straightforward idea is to use Dynamic Time Warping (DTW) to compare the similarity of the obtained spatial-temporal phase profile with the referenced trough zone, which is illustrated in STPP [49]. However, DTW algorithm is time consuming. The computational complexity of DTW algorithm is $O(\frac{NM}{w^2})$, where w denotes the size of sliding window. N and M denote the length of measured and referenced phase profile respectively. Let's assume we have n nanodrones in the swarm. To detect all the trough zones, the overall computational complexity is $O(\frac{3nNM}{w^2})$, since we need to predict the relative position along x, y and z axis. As we can see, the high computational complexity will introduce high processing latency. So, we use the approach proposed in Taggo [22] to achieve fast trough zone detection with computational complexity of $O(N)$, where N is the length of the phase profile. The main idea is to use a sliding window to go over the phase profile once as shown in Fig. 14, thereby we can leverage the structure of the phase profile for trough zone detection. The trough zone can be found between two consecutive jumping points. Since we just go over the phase profile once, the overall computational complexity is $O(3(nN))$.

Algorithm 1 Relative Positioning Algorithm

Require:
- Commodity RFID passive system and nanodrone swarm;

Ensure:
- The relative position of nanodrones in the swarm;

1: **for** $i \in \{x, y, z\}$ **do**
2:     Profiling the spatial-temporal phase profiles along i axis with Equation (1);
3:     Detecting and splicing trough zones with Equation (3);
4:     Predicting the relative positions of nanodrones with Equation (4);
5: **end for**
6: **return** The relative positions of the nanodrones in the swarm;

---

2) Relative Localization.: As we can see, the spatial-temporal phase profile consists of one trough zone and multiple discontinuous parts due to the modular operation. To achieve fast and accurate relative localization, we splice the discontinuous parts together with the trough zone as shown in Fig. 15 with the flowing equation [22]:

$$\theta_i = \begin{cases} \theta_i - \left\lceil \frac{\theta_i - \theta_{i-1}}{2\pi} \right\rceil 2\pi, & \theta_i - \theta_{i-1} > \pi \\ \theta_i + \left\lceil \frac{\theta_i - \theta_{i-1}}{2\pi} \right\rceil 2\pi, & \theta_i - \theta_{i-1} < -\pi \\ \theta_i, & otherwise \end{cases} \tag{3}$$

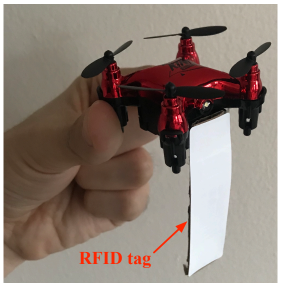

Fig. 16: Commodity passive RFID tagged nanodrone.

Fig. 17: **Nanodrone swarm.** There are five nanodrones in the swarm. Three Holyton HT02 Mini Drones [6] and two Masefu Mini Drones [7]

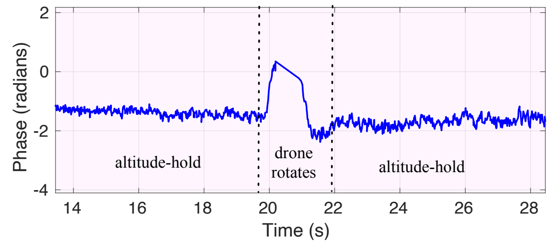

Fig. 18: When the RFID-tagged nanodrone rotates/flips, the signal phase significantly changes. However, when the RFID-tagged nanodrone holds its altitude, the signal phase maintains constant.

where θ_i indicates the i-th phase value. After we obtain the spliced phase reading over time, we can detect the time ordering of the trough's lowest point to predict the relative position of nanodrones in the swarm. To detect the trough's lowest point, we just need to go over the spliced trough zone once using the following equation:

$$d_{ix} = t, \, if \, \theta_t < \theta_{t-1} \, and \, \theta_t < \theta_{t+1} \tag{4}$$

where d_{ix} denotes the time when the trough's lowest point is achieved for nanodrone i flying along x axis. Note, d_{ix} is the global smallest point due to the trough shape of spliced phase profile. To predict the relative position of the nanodrones along x axis, we can compare the value of $d_{ix}, i \in \{1, 2, ..., n\}$. The smaller value of d_{ix} is, the closer nanodrone is to the reader's antenna.

We summarize the procedure of relative positioning algorithm in 1, which contains three main steps. The first step is profiling the spatial-temporal phase profile. Then, we detect and splice the trough zone together with the adjacent parts in the profile. At last, we can predict the relative position of nanodrones in the swarm.

V. Implementation and Evaluation

In this section, we present the general implementation and evaluation details of RFDrone's prototype. The details for the specific experiments and the corresponding results will be illustrated in the next section.

RFID Reader. We adopt USRP N210 radio as the RFID reader developed in the prior work [28], which is instrumented with SBX daughter board to interrogate the tags. It is compatible with FCC regulation using EPC Gen2 standard for UHF RFID communication at frequency band between 902-928MHz. The reader instrumented with the directional antennas will activate and interrogate the tags using slotted ALOHA protocol. During experiments, we will just extract the channel state information (specifically, the phase readings over time) for nanodrone relative localization in the swarm.

RFID Tag. We use the general-purpose commodity passive RFID tags (e.g., Alien Squiggle RFID tag ALN-9640 [1], ALN-9762 [3] and ALN-9662 [2]) to evaluate RFDrone's performance. Each tag is low-cost with price of around 5 cents, which will enable the ubiquitous sensing.

Nanodrone Swarm. The nanodrone swarm consists of multiple nanodrones. In our prototype, we use up to five nanodrones (e.g., three Holyton HT02 Mini Drones [6] and two Masefu Mini Drones [7]) to formulate a nanodrone swarm as shown in Fig. 17, and each nanodrone is attached with one RFID tag as shown in Fig. 16. Each individual nanodrone has three speed modes: low speed mode of around $0.15m/s$, medium speed mode of around $1m/s$ and high speed mode of around $2m/s$. During the experiments, each individual nanodrone in the swarm is controlled by the remote controller. The adjacent nanodrones will be separated by half wavelength away to avoid the tag-tag coupling effect for the safe platooning.

Experimental Settings. The reader will connect with the PC host (i.e., HP laptop running Ubuntu 16.04 operating system) through Ethernet cables. We use USRP N210 as the RFID reader to interrogate the tags and extract the backscattered channel between each RFID-tagged nanodrone and the reader's antenna. The reader is responsible to collect the backscattered signals, which will be further forwarded to the PC host and processed with MATLAB in PC host. After we obtain the backscattered channel, we run relative localization algorithm in MATLAB.

We evaluate the performance of RFDrone in indoor and outdoor environments (e.g., apartment room and office room) with up to five nanodrones. The indoor environment is a rich scattering environment with different furniture around (e.g., desks, chairs and sofas). The distance between the nanodrone swarm and the reader's antenna is around 1.5 meters within the reader's communication range by default. We control them through the remote controller. In default, we control the nanodrone swarm to fly in the low-speed mode. In the results section, we will measure the impact of different system settings on RFDrone's performance such as reader-tag distance, flying speed and different nanodrone swarm patterns.

VI. Results

A. *Effectiveness of Noise Filtering*

Since the nanodrone is a mechanical system, its body shift, rotation flip or vibration will change the backscattered signals as the RFID tag is attached to nanodrone's body. To see this clearly, we do an experiment to show the variation of phase readings over time from an RFID-tagged nanodrone.

Method. We fly a nanodrone attached with a commodity passive RFID tag. Then, we control the nanodrone to rotate to measure its impact on phase readings over time. We expect to see the significant variation of phase readings, as the nanodrone flips or rotates.

Result. As shown in Fig. 18, when the nanodrone holds its altitude (i.e., hovering in the sky), the signal phase is quite stable. When the nanodrone's body rotates, the signal phase changes significantly. This indicates that the nanodrone's body vibration will not affect the backscattered signals significantly. So, we can ignore the nanodrone's body vibration in our analysis. But, the nanodrone's body shift/rotation can significantly affect the backscattered signals, which needs to be filtered out.

VII. Conclusion

In this paper, we propose RFDrone, a system that can sense the relative position of the nanodrones in the swarm, using the commodity passive RFID tags. To do so, we attach commodity passive RFID tag on each nanodrone, such that the relative position of the nanodrones in the swarm can be estimated through the time ordering of trough's lowest point in the spatial and temporal phase profile. We believe RFDrone can proliferate the human-drone interaction, dazzling drone show for entertainment industry and safe drone swarm platooning.

References

[1] Alien squiggle rfid white wet inlay (aln-9640, higgs-3), 2020. URL https://www.atlasrfidstore.com/alien-squiggle-rfid-white-wet-inlay-aln-9640-higgs-3/.

[2] Alien short rfid white wet inlay (aln-9662, higgs-3), 2020. URL https://www.atlasrfidstore.com/alien-short-rfid-white-wet-inlay-aln-9662-higgs-3/.

[3] Alien short rfid white wet inlay (aln-9762, higgs-4), 2020. URL https://www.atlasrfidstore.com/alien-short-rfid-white-wet-inlay-aln-9762-higgs-4/.

[4] Dazzling drone show with lights, 2020. URL https://skymagic.show/.

[5] Mini drone fy804 4ch 2.4g 6axis 360 degree roll mini helicopter led plane model toys rc aircraft, 2020. URL https://www.aliexpress.com/i/32983575363.html.

[6] Holyton ht02 mini drone, 2020. URL https://www.amazon.com/Holyton-Beginners-Quadcopter-Batteries-Protection/dp/B08DNSYT2L.

[7] Masefu mini drone, 2020. URL https://www.amazon.com/Masefu-Helicopter-Quadcopter-Trajectory-Programming.

[8] Parastoo Abtahi, David Y Zhao, Jane L E, and James A Landay. Drone near me: Exploring touch-based human-drone interaction. *Proceedings of the ACM on Interactive, Mobile, Wearable and Ubiquitous Technologies*, 1 (3):1–8, 2017.

[9] Adeola Bannis, Hae Young Noh, and Pei Zhang. Bleep: motor-enabled audio side-channel for constrained uavs. In *Proceedings of the 26th Annual International Conference on Mobile Computing and Networking*, pages 1–13, 2020.

[10] Tara Boroushaki, Junshan Leng, Ian Clester, Alberto Rodriguez, and Fadel Adib. Robotic grasping of fully-occluded objects using rf perception. In *2021 IEEE International Conference on Robotics and Automation (ICRA)*, pages 923–929. IEEE, 2021.

[11] Tara Boroushaki, Isaac Perper, Mergen Nachin, Alberto Rodriguez, and Fadel Adib. Rfusion: Robotic grasping via rf-visual sensing and learning. In *Proceedings of the 19th ACM Conference on Embedded Networked Sensor Systems*, pages 192–205, 2021.

[12] Daren C Brabham. *Crowdsourcing*. Mit Press, 2013.

[13] Ayon Chakraborty, Eugene Chai, Karthikeyan Sundaresan, Amir Khojastepour, and Sampath Rangarajan. Skyran: A self-organizing lte ran in the sky. In *Proceedings of the 14th International Conference on emerging Networking EXperiments and Technologies*, pages 280–292, 2018.

[14] Mo Chen, Qie Hu, Casey Mackin, Jaime F Fisac, and Claire J Tomlin. Safe platooning of unmanned aerial vehicles via reachability. In *2015 54th IEEE Conference on Decision and Control (CDC)*, pages 4695–4701. IEEE, 2015.

[15] Titus Cieslewski, Siddharth Choudhary, and Davide Scaramuzza. Data-efficient decentralized visual slam. In *2018 IEEE international conference on robotics and automation (ICRA)*, pages 2466–2473. IEEE, 2018.

[16] Travis Deyle, Cressel Anderson, Charles C Kemp, and Matthew S Reynolds. A foveated passive uhf rfid system for mobile manipulation. In *2008 IEEE/RSJ International Conference on Intelligent Robots and Systems*, pages 3711–3716. IEEE, 2008.

[17] Travis Deyle, Hai Nguyen, Matt Reynolds, and Charles C Kemp. Rf vision: Rfid receive signal strength indicator (rssi) images for sensor fusion and mobile manipulation. In *2009 IEEE/RSJ International Conference on Intelligent Robots and Systems*, pages 5553–5560. IEEE, 2009.

[18] Travis Deyle, Christopher J Tralie, Matthew S Reynolds, and Charles C Kemp. In-hand radio frequency identification (rfid) for robotic manipulation. In *2013 IEEE International Conference on Robotics and Automation*, pages 1234–1241. IEEE, 2013.

[19] Travis Deyle, Matthew S Reynolds, and Charles C Kemp. Finding and navigating to household objects with uhf rfid tags by optimizing rf signal strength. In *2014 IEEE/RSJ International Conference on Intelligent Robots and Systems*, pages 2579–2586. IEEE, 2014.

[20] Duarte Dias, Rodrigo Ventura, Pedro Lima, and Alcherio Martinoli. On-board vision-based 3d relative localization system for multiple quadrotors. In *2016 IEEE International Conference on Robotics and Automation (ICRA)*, pages 1181–1187. Ieee, 2016.

[21] Xintong Du, Carlos E Luis, Marijan Vukosavljev, and Angela P Schoellig. Fast and in sync: Periodic swarm patterns for quadrotors. In *2019 International Conference*

on Robotics and Automation (ICRA), pages 9143–9149. IEEE, 2019.

[22] Chunhui Duan, Jiajun Liu, Xuan Ding, Zhenhua Li, and Yunhao Liu. Full-dimension relative positioning for rfid-enabled self-checkout services. *Proceedings of the ACM on Interactive, Mobile, Wearable and Ubiquitous Technologies*, 5(1):1–23, 2021.

[23] Ming Gao, Feng Lin, Weiye Xu, Muertikepu Nuermaimaiti, Jinsong Han, Wenyao Xu, and Kui Ren. Deaf-aid: mobile iot communication exploiting stealthy speaker-to-gyroscope channel. In *Proceedings of the 26th Annual International Conference on Mobile Computing and Networking*, pages 1–13, 2020.

[24] Antonio Gomes, Calvin Rubens, Sean Braley, and Roel Vertegaal. Bitdrones: Towards using 3d nanocopter displays as interactive self-levitating programmable matter. In *Proceedings of the 2016 CHI Conference on Human Factors in Computing Systems*, pages 770–780, 2016.

[25] Mahanth Gowda, Justin Manweiler, Ashutosh Dhekne, Romit Roy Choudhury, and Justin D Weisz. Tracking drone orientation with multiple gps receivers. In *Proceedings of the 22nd annual international conference on mobile computing and networking*, pages 280–293, 2016.

[26] Wail Gueaieb and Md Suruz Miah. An intelligent mobile robot navigation technique using rfid technology. *IEEE Transactions on Instrumentation and Measurement*, 57 (9):1908–1917, 2008.

[27] Unsoo Ha, Junshan Leng, Alaa Khaddaj, and Fadel Adib. Food and liquid sensing in practical environments using rfids. In *17th {USENIX} Symposium on Networked Systems Design and Implementation ({NSDI} 20)*, pages 1083–1100, 2020.

[28] Nikos Kargas, Fanis Mavromatis, and Aggelos Bletsas. Fully-coherent reader with commodity sdr for gen2 fm0 and computational rfid. *IEEE Wireless Communications Letters*, 4(6):617–620, 2015.

[29] Myungsik Kim and Nak Young Chong. Direction sensing rfid reader for mobile robot navigation. *IEEE Transactions on Automation Science and Engineering*, 6(1):44–54, 2008.

[30] Ming-Yu Liu, Oncel Tuzel, Ashok Veeraraghavan, Yuichi Taguchi, Tim K Marks, and Rama Chellappa. Fast object localization and pose estimation in heavy clutter for robotic bin picking. *The International Journal of Robotics Research*, 31(8):951–973, 2012.

[31] Giuseppe Loianno, Chris Brunner, Gary McGrath, and Vijay Kumar. Estimation, control, and planning for aggressive flight with a small quadrotor with a single camera and imu. *IEEE Robotics and Automation Letters*, 2(2):404–411, 2016.

[32] Chris Xiaoxuan Lu, Muhamad Risqi U Saputra, Peijun Zhao, Yasin Almalioglu, Pedro PB de Gusmao, Changhao Chen, Ke Sun, Niki Trigoni, and Andrew Markham. milliego: single-chip mmwave radar aided egomotion estimation via deep sensor fusion. In *Proceedings of the 18th Conference on Embedded Networked Sensor Systems*, pages 109–122, 2020.

[33] Zhihong Luo, Qiping Zhang, Yunfei Ma, Manish Singh, and Fadel Adib. 3d backscatter localization for fine-grained robotics. In *16th {USENIX} Symposium on Networked Systems Design and Implementation ({NSDI} 19)*, pages 765–782, 2019.

[34] Yunfei Ma, Nicholas Selby, and Fadel Adib. Drone relays for battery-free networks. In *Proceedings of the Conference of the ACM Special Interest Group on Data Communication*, pages 335–347, 2017.

[35] Yunfei Ma, Nicholas Selby, and Fadel Adib. Minding the billions: Ultra-wideband localization for deployed rfid tags. In *Proceedings of the 23rd Annual International Conference on Mobile Computing and Networking*, pages 248–260, 2017.

[36] Mani Monajjemi, Sepehr Mohaimenianpour, and Richard Vaughan. Uav, come to me: End-to-end, multi-scale situated hri with an uninstrumented human and a distant uav. In *2016 IEEE/RSJ International Conference on Intelligent Robots and Systems (IROS)*, pages 4410–4417. IEEE, 2016.

[37] Eduardo Montijano, Eric Cristofalo, Dingjiang Zhou, Mac Schwager, and Carlos Saguees. Vision-based distributed formation control without an external positioning system. *IEEE Transactions on Robotics*, 32(2):339–351, 2016.

[38] Mehrdad Moradi, Karthikeyan Sundaresan, Eugene Chai, Sampath Rangarajan, and Z Morley Mao. Skycore: Moving core to the edge for untethered and reliable uav-based lte networks. In *Proceedings of the 24th Annual International Conference on Mobile Computing and Networking*, pages 35–49, 2018.

[39] Wai Shan Ng and Ehud Sharlin. Collocated interaction with flying robots. In *2011 Ro-Man*, pages 143–149. IEEE, 2011.

[40] Kei Nitta, Keita Higuchi, and Jun Rekimoto. Hoverball: augmented sports with a flying ball. In *Proceedings of the 5th Augmented Human International Conference*, pages 1–4, 2014.

[41] Mohammad Obaid, Felix Kistler, Gabrielė Kasparavičiūtė, Asim Evren Yantaç, and Morten Fjeld. How would you gesture navigate a drone? a user-centered approach to control a drone. In *Proceedings of the 20th International Academic Mindtrek Conference*, pages 113–121, 2016.

[42] Sunhong Park and Shuji Hashimoto. Autonomous mobile robot navigation using passive rfid in indoor environment. *IEEE Transactions on industrial electronics*, 56(7):2366–2373, 2009.

[43] Maxim Pavliv, Fabrizio Schiano, Christopher Reardon, Dario Floreano, and Giuseppe Loianno. Tracking and relative localization of drone swarms with a vision-based headset. *IEEE Robotics and Automation Letters*, 6(2): 1455–1462, 2021.

[44] Fabrizio Schiano and Paolo Robuffo Giordano. Bearing rigidity maintenance for formations of quadrotor uavs.

In *2017 IEEE International Conference on Robotics and Automation (ICRA)*, pages 1467–1474. IEEE, 2017.

[45] Fabrizio Schiano and Roberto Tron. The dynamic bearing observability matrix nonlinear observability and estimation for multi-agent systems. In *2018 IEEE International Conference on Robotics and Automation (ICRA)*, pages 3669–3676. IEEE, 2018.

[46] Judy Scott and Carlton Scott. Drone delivery models for healthcare. In *Proceedings of the 50th Hawaii international conference on system sciences*, 2017.

[47] Longfei Shangguan and Kyle Jamieson. The design and implementation of a mobile rfid tag sorting robot. In *Proceedings of the 14th annual international conference on mobile systems, applications, and services*, pages 31–42, 2016.

[48] Longfei Shangguan and Kyle Jamieson. Leveraging electromagnetic polarization in a two-antenna whiteboard in the air. In *Proceedings of the 12th International on Conference on emerging Networking EXperiments and Technologies*, pages 443–456, 2016.

[49] Longfei Shangguan, Zheng Yang, Alex X Liu, Zimu Zhou, and Yunhao Liu. Relative localization of {RFID} tags using spatial-temporal phase profiling. In *12th {USENIX} Symposium on Networked Systems Design and Implementation ({NSDI} 15)*, pages 251–263, 2015.

[50] Longfei Shangguan, Zimu Zhou, and Kyle Jamieson. Enabling gesture-based interactions with objects. In *Proceedings of the 15th Annual International Conference on Mobile Systems, Applications, and Services*, pages 239–251, 2017.

[51] Roberto Tron, Justin Thomas, Giuseppe Loianno, Kostas Daniilidis, and Vijay Kumar. A distributed optimization framework for localization and formation control: Applications to vision-based measurements. *IEEE Control Systems Magazine*, 36(4):22–44, 2016.

[52] Markus Waibel, Bill Keays, and Federico Augugliaro. Drone shows: Creative potential and best practices. Technical report, ETH Zurich, 2017.

[53] Viktor Walter, Nicolas Staub, Antonio Franchi, and Martin Saska. Uvdar system for visual relative localization with application to leader–follower formations of multirotor uavs. *IEEE Robotics and Automation Letters*, 4(3): 2637–2644, 2019.

[54] Jingxian Wang, Junbo Zhang, Rajarshi Saha, Haojian Jin, and Swarun Kumar. Pushing the range limits of commercial passive rfids. In *16th {USENIX} Symposium on Networked Systems Design and Implementation ({NSDI} 19)*, pages 301–316, 2019.

[55] Ju Wang, Liqiong Chang, Shourya Aggarwal, Omid Abari, and Srinivasan Keshav. Soil moisture sensing with commodity rfid systems. In *Proceedings of the 18th International Conference on Mobile Systems, Applications, and Services*, pages 273–285, 2020.

[56] Jue Wang and Dina Katabi. Dude, where's my card? rfid positioning that works with multipath and non-line of sight. In *Proceedings of the ACM SIGCOMM 2013 conference on SIGCOMM*, pages 51–62, 2013.

[57] Jue Wang, Fadel Adib, Ross Knepper, Dina Katabi, and Daniela Rus. Rf-compass: Robot object manipulation using rfids. In *Proceedings of the 19th annual international conference on Mobile computing & networking*, pages 3–14, 2013.

[58] Jue Wang, Deepak Vasisht, and Dina Katabi. Rf-idraw: virtual touch screen in the air using rf signals. *ACM SIGCOMM Computer Communication Review*, 44(4): 235–246, 2014.

[59] Gang Xiang, Andrew Hardy, Mohammed Rajeh, and Lahari Venuthurupalli. Design of the life-ring drone delivery system for rip current rescue. In *2016 IEEE Systems and Information Engineering Design Symposium (SIEDS)*, pages 181–186. IEEE, 2016.

[60] Daniel Zelazo, Antonio Franchi, Heinrich H Bülthoff, and Paolo Robuffo Giordano. Decentralized rigidity maintenance control with range measurements for multi-robot systems. *The International Journal of Robotics Research*, 34(1):105–128, 2015.

[61] Yongpan Zou, Jiang Xiao, Jinsong Han, Kaishun Wu, Yun Li, and Lionel M Ni. Grfid: A device-free rfid-based gesture recognition system. *IEEE Transactions on Mobile Computing*, 16(2):381–393, 2016.